Demonstration of Three-Dimensional DNA Trapping using Electric Force and Hydrodrag Force

Yoshiaki Ukita, Lassoued Mouez, Yuichi Tomizawa, and Yuzuru Takamura

School of Materials Science, Japan Advanced Institute of Science and Technology (JAIST)

Nomi, Ishikawa 923-1292, Japan

Abstract

This paper describes the first demonstration of DNA trapping in a stacked three-dimensional (3D) microchannel. To carry out the 3D trapping of DNA by using electric force and hydrodrag force, a 3D microchip with a stacked structure is fabricated by the conventional rapid prototyping process and SU-8 peel-off process. Experimental results show that DNA trapping is observed on the application of electric potential with continuous pumping of DNA, but it is not observed in the absence of an electric potential. Further, the results suggest that the trapping throughput of DNA clearly depends on the capillary diameter but not on the flow rate. Thus, we conclude that, for a constant trapping area, reduction in the size of capillary structures with a high density results in an increase in the efficiency of DNA trapping.

1. Introduction

The integration of sample preparation processes such as cell separation, extraction of DNA from cells, and purification and amplification of DNA on a single microchip is important to realize the next-generation microchip-based chemical systems for performing biological experiments [1-12]. Microchip-based DNA extraction has been proposed by using solid-phase extraction (SPE), which is a simple miniaturization of the conventional method [4-12]. Although the conventional SPE has been downscaled successfully, there still remain some issues to be addressed. The improvement of the yield is difficult because the efficiency of DNA extraction depends on two factors: (1) the rate of DNA capture into the solid phase and (2) the rate of recovery of DNA from the solid phase. Multi-step operations and a long washing time are necessary to increase the purity of the DNA requires longtime consumption of the process. To realize further simple and efficient DNA extraction and concentration, miniaturization to micro-scale is necessary.

We have demonstrated DNA trapping in microchannels [13-18]. Various charged molecules or cells are trapped by the hydrodrag force and electric force in the microchannel with a size of 1 to 10 μm, as shown in Fig. 1 [17]. It is interesting to note that this method does not require any solid phase to adsorb the DNA molecules, because they are directly trapped in the triangular microchannel under continuous flow by the balance between the hydrodrag force and electric force. Trapped DNA is immediately released and recovered by eliminating one of the forces, which induces trapping. Considering the application of DNA trapping to practical use such as purification and concentration of DNA molecules, it is expected that the extraction yield of conventional SPE can be improved because the yield of DNA extraction depends only on the

efficiency of trapping, and the trapping probability can become nearly 100% under optimized conditions [17].

For improvement of the total trapping throughput of DNA for practical applications, it is necessary to realize large-scale integration of trapping microchannels. However, the area, and thus the integration density, of planar microchips is limited. However, trapping has been demonstrated by using a conventional planar microchannel. To increase the total throughput of DNA trapping, increasing the trapping efficiency using highly integrated trapping microchannels is necessary. The use of a three-dimensional (3D) structure is one of the most efficient ways to integrate the channels with a high density [19-25]. Thus, this paper focuses on the first demonstration of DNA trapping in a 3D trapping channel formed in the membrane of a photoresist (SU-8) film.

2. Simulation and Experiment

2.1 Simulation method

To evaluate the feasibility of 3D trapping, a numerical simulation was carried out by using COMSOL multiphysics software. A model consisting of seven cylindrical capillaries with a diameter of 100 μm and length of 100 μm was designed. The capillaries were stacked on a planar microchannel with a height of 50 μm and connected to the inlet and outlet having a rectangular cross section of 50 × 100 μm^2 (see Fig. 4). The inlet and outlet pressures were set at 400 and 0 Pa, respectively. The electric potentials of the inlet and outlet were set at 0 and 50 V, respectively.

2.2 Microchip design and fabrication

The microchip with a stacked structure, which consists of the SU-8 film with a vertical

capillary structure and a poly(dimethylsiloxane) (PDMS) planar structure, was fabricated as shown in Fig. 2. The photomasks used to pattern the cylindrical vertical capillaries with 10 integrated holes having a diameter of 50 μm (type A) and 27 integrated holes having a diameter of 30 μm (type B) were designed to form a diamond pattern on the film. To create through holes in the SU-8 film, the Si substrate was coated with a releasing agent (Omnicoat Microchem) and baked at 200 ^{o}C for 1 min. Then, the substrate was coated with an SU-8 film (SU-8 3035 Microchem) having a thickness of 50 μm and soft-baked at 95 ^{o}C for 15 min. The SU-8 film was exposed to UV light for 15 s (corresponding to 150 mJ/cm^2) and then post-baked at 95 ^{o}C for 5 min. The pattern was developed by using SU-8 developer (Microchem). The SU-8 film was naturally released from the substrate when the developing solution reached the surface of the substrate. After which, the released SU-8 film was rinsed in isopropyl alcohol and dried naturally. The patterned through-hole structure was observed using a confocal laser microscope (KEYENCE VK9710), and the diameter was measured to be in the range of 22 μm to 62 μm. No deformation of the pattern was observed except for the difference in the diameter of the holes. The PDMS layer was prepared by using conventional rapid prototyping method [26]. The mold used for the replication of the microchannel was patterned on the Si substrate using an SU-8 film with a thickness of 50 μm. PDMS was poured onto the mold up to a thickness of 1.5 mm and cured in a convection oven at 75 ^{o}C for 1.5 h. The holes for the inlet and outlet port were punched on the upper side of the PDMS layer, and the layer was attached to the glass substrate using a silicone rubber tube and Pt electrodes. Finally, the SU-8 film and the bottom PDMS layer were aligned and stacked to perform the experiment.

2.3 Trapping experiments

2.3.1 Reagents

The samples for the experiments were prepared as follows. 0.5x tris(borate ethyldiamineteraacetic) acid (0.5x TBE, pH 8.2) buffer containing 2.4 mg/ml of glucose, 20 µg/ml of catalase, and 0.1 mg/ml of glucose oxidase was prepared for the prevention of fragmentation of DNA because of dissolved oxygen. A commercially available DNA (Nippon Gene T4 DNA 166 kbp) sample was dissolved in the prepared 0.5x TBE buffer with a fluorescence dye (Molecular Probe YOYO-1) such that the ratio of the YOYO-1 molecules to the DNA sample was 5:1 (i.e., 60 pM of T4 DNA and 2 µM of YOYO-1) and was incubated for 24 h. Dyed DNA was dissolved in 0.5x TBE buffer containing 0.3% (w/w) of poly(vinyl pyrrolidone) (PVP), 4% (v/v) of 2-mercaptoethanol, 2.4 mg/ml of glucose, 20 µg/ml of catalase, and 0.1 mg/ml of glucose oxidase for preventing electro-osmosis and fragmentation of DNA because of dissolved oxygen.

2.3.2 Trapping experimental set-up and procedure

As shown in fig. 3, the fabricated chip was attached to the tube and Pt electrode connectors; and the inlet tube was connected to the microsyringe (Hamilton GASTIGHT 1750), which was attached to the microsyringe pump (EiCOM ESP-64). The end of the outlet tube was connected to an Eppendorf tube to collect the waste. To induce the electric force, in a direction opposite to the flow, the inlet and outlet Pt electrodes were connected to the positive and negative channel of a DC power source, respectively. The chip was set on a fluorescence microscope system such that its bottom side faced the objective lens. To initialize the trapping experiment, the entire channel was filled with the sample and the flow rate of the sample was kept stable at the

required value. Finally, the required electric potential was applied.

3. Results and Discussion

3.1 Simulation results

Figure 4 shows the image of the total force field obtained by simulation. The color contours indicate the magnitude of the total force, and the direction and length of the red arrow indicate the direction and magnitude of the total force, respectively. The orbit of the DNA is simulated and indicated by the streamline, and the characteristic swirl orbit is simulated around the edges of the vertical capillary as shown in Fig. 4(b). It is known that DNA trapping is observed where the hydrodrag force and the electric force balance each other [16, 18]. As shown in Fig. 4(b), minimal force is expected around the edge of the inlet and outlet of the vertical capillaries. It is expected that trapping will be observed around the swirl orbit of the streamline.

3.2 Demonstration of three-dimensional DNA trapping

We carried out the trapping experiment by using the fabricated 3D trapping chips. Figure 5 shows fluorescence microscope images obtained from the experiments by using type B capillary structure and a sample flow rate of 1.000 μl/min. While significant fluorescence was not observed under a relatively low electric voltage of 50 V, clear fluorescence was observed around the edge of the trapping capillaries under voltages greater than 100 V. While no trapping was observed in the absence of an electric potential and continuous pumping of the DNA sample solution, DNA trapping was successfully observed around the edge of the trapping capillaries. The trapped DNA was released by turning off the voltage. The back stream of the DNA, which originated

because of electro-osmotic flow (EOF), was observed on the surface of the SU-8 film for voltages larger than 150 V. While the trapping pattern appeared relatively uniform under 100 V, an inhomogeneous trapping pattern was observed at a voltage of 200 V. It is notable that trapping was observed along the edge of the structure. This agreed well with the simulation result. The observed trapping was expected to be induced around the balanced force field of the two forces: electric force and hydrodrag force. Thus, we successfully demonstrated DNA trapping. The result offers two important possibilities: (1) 3D trapping by using a vertically stacked trapping capillary structure and (2) the use of SU-8 microstructures. These possibilities are important, because the realization of the stacking concept offers various benefits such as high- throughput trapping, development of high-performance systems with integration of multiple modules, and automatic parallel operation of multiple systems realized by stacking and integrating 3D microchannel network structures [19-25, 27]. Moreover, the use of polymer structure is cost-effective because of the convenience of mass production by photolithography. DNA trapping has been demonstrated by using other materials such as glass or PDMS, which is not suitable for fabricating 3D trapping channel structures.

3.3 Effect of parameters on trapping efficiency

The fluorescence images are analyzed by using SIMPLE-PCI software (Leeds Instruments) to convert the trapped amount of DNA to fluorescence intensity. Figure 6 shows the obtained time shift of the fluorescence intensity. Figures 6(a) and 6(b) are taken by using type A capillary chip and voltage range with different flow rate with 1.000 and 2.942 μl/min, respectively. While the sample DNA is supplied by continuous pumping, the fluorescence intensity typically saturates in an elapsed time of 200 s. It is

considered that the saturation of the fluorescence intensity with continuous supply of the DNA sample suggests the equilibrium state of the trapping and releasing of DNA molecules, and this state defines the maximum trapping or capacity of DNA trapping. Next, to estimate the optimal trapping voltage conditions for the maximum trapping, fluorescence intensity from 300 to 600 s is averaged and the relation with applied voltages is shown in Fig. 7. As shown in Fig. 7, fluorescence intensity peaks are observed at 200 and 300 V. The slight increase of peak voltage with flow rate can be understood reasonably from the balance of hydrodrag force and electric force. It is notable that the clear difference of peak fluorescence intensity is not found due to the difference of flow rate. The slope of 200 V line of Fig. 6(a) and 300 V of Fig. 6(b) are calculated to estimate the trapping rate. The slope of the fluorescence intensity is calculated to be between 0 and 100 s. It is found that the trapping rate is also the same under optimal trapping conditions by comparing slopes (41.2 and 41.6 s^{-1}). By considering these results, it is suggested that the efficiency of the trapping does not increase with the sample pumping rate and it seems better to have a low flow rate of sample to increase the trapping rate, since the passing rate of DNA will increase with the flow rate under the same trapping rate, while it is considered to be different with thinner concentration of sample.

Next, Fig. 6(c) shows the fluorescence intensity change along the elapsed time of DNA trapping by using type B capillary structure with flow rate of 1.000 μl/min, which corresponds to the same mean flow velocity with the condition as shown in Fig. 6(b). While the curve of fluorescence in Fig. 6(c) seems to be increasing, the fluorescence from 300 to 600 s is also averaged and plotted on Fig. 7 for comparison. The result shows the higher trapping throughput at the peak of fluorescence intensity. However, by

dividing the peak fluorescence intensity by the integrated number of capillaries, it becomes 70% of type A, suggesting the lower or no-significant improvement of efficiency of the DNA trapping per capillary. On the other hand, it increases by 5.6 times when the fluorescence intensity is divided by the cross section area. Thus, the smaller capillary provides higher trapping throughput per same area size. In conclusion, smaller capillary structures with higher density result in higher throughput of trapping by considering same size of trapping area.

4. Conclusions

In this paper, we have described the demonstration of DNA trapping by using a 3D SU-8 microstructure. The successful demonstration of DNA trapping using the 3D microstructure suggests the possibility of further improvement of trapping efficiency by using a 3D array structure of trapping channels. It is also notable that trapping has been demonstrated by using a polymer (SU-8) structure, because it offers the possibility of mass production of devices with the cost-effective photolithography process. This study has presented evidence for the practicality of SU-8 3D structure for DNA trapping. This paper has also discussed some basic characteristics of DNA trapping. As the results show, clear dependence of the trapping efficiency on trapping conditions such as flow rate and electric potential has not been found, while strong dependence on the capillary structure has been found. Finally, we have developed the simple concept of *smaller capillary with higher density* for the optimization of the trapping capillary.

References

[1] P. K. Yuen, L. J. Kricka, P. Fortina, N. J. Panaro, T. Sakazume, and P. Wilding: Genome Res. **11** (2001) 405.

[2] D. Erickson, and D. Li: Anal. Chim. Acta **507** (2004) 11.

[3] R. Pal, M. Yang, R. Lin, B. N. Johnson, N. Srivastava, S. Z. Razzacki, K. J. Chomistek, D. C. Heldsinger, R. M. Haque, V. M. Ugaz, P. K. Thwar, Z. Chen, K. Alfano, M. B. Yim, M. Krishnan, A. O. Fuller, R. G. Larson, D. T. Burke, and M. A. Burns: Lab Chip **5** (2005) 1024.

[4] X. Chen, D. Cui, C. Liu, H. Li, and J. Chen: Anal. Chim. Acta **587** (2007) 237.

[5] Y. Huang, S. Joo, M. Duhon, M. Heller, B. Wallace, and X. Xu: Anal. Chem. **74** (2002) 3362.

[6] C. M. Chang, S. K. Hsiung, and G. B. Lee: Jpn. J. Appl. Phys. **46** (2007) 3126.

[7] J. G. Lee, K. H. Cheong, N. Huh, S. Kim, J. W. Choi, and C. Ko: Lab Chip **6** (2006) 886.

[8] K. A. Wolfe, M. C. Breadmore, J. P. Ferrance, M. E. Power, J. F. Conroy, P. M. Norris, and J. P. Landers: Electrophoresis **23** (2002) 727.

[9] J. M. Bienvenue, N. Duncalf, D. Marchiarullo, J. P. Feffance, and J. P. Landers: J. Forensic Sci. **51** (2006) 266.

[10] M. C. Breadmore, K. A. Wolfe, I. G. Arcival, W. K. Leung, D. Dickson, B. C. Giordano, M. E. Power, J. P. Ferrance, S. H. Feldman, P. M. Norris, and J. P. Landers: Anal. Chem. **75** (2003) 1880.

[11] T. Nakagawa, T. Tanaka, D. Niwa, T. Osaka, H. Takayama, and T. Matsunaga: J. Biotechnol. **116** (2005) 105.

[12] Z. Long, Z. Shen, D. Wu, J. Qin, and B. Lin: Lab Chip **7** (2007) 1819.

[13] Y. Takamura, T. Havama, M. Ueda, Y. Baba, and Y. Horiike: Proc. μTAS 2002 **1** (2002) 317.

[14] Y. Takamura, Y. Horiike, Y. Baba, and E. Tamiya: Proc. μTAS 2003 **1** (2003) 317.

[15] Y. Tomizawa, K. Yuhki, Y. Morita, E. Tamiya, and Y. Takamura: Proc. μTAS 2004 **1** (2004) 659.

[16] K. Ueno, W. Nagasaka, Y. Tomizawa, Y. Nakamori, E. Tamiya, and Y. Takamura: Jpn. J. Appl. Phys. **46** (2007) 5358.

[17] Y. Tomizawa, E. Tamiya, and Y. Takamura: Phys. Rev. E **79** (2009) 051902.

[18] Y. Tomizawa et al: preparation for publication.

[19] Y. Utsumi, T. Asano, Y. Ukita, K. Matsui, M. Takeo, and S. Negoro: Jpn. J. Appl. Phys. **44** (2005) 5707.

[20] Y. Utsumi, T. Asano, Y. Ukita, K. Matsui, M. Takeo, and S. Negoro: J. Vac. Sci. Technol. B **24** (2006) 2606.

[21] Y. Ukita, T. Asano, K. Fujiwara, T. Yokoyama, K. Matsui, M. Takeo, S. Negoro, T. Saiki, and Y. Utsumi: Jpn. J. Appl. Phys. **45** (2006) 7203.

[22] Y. Ukita, T. Asano, K. Fujiwara, K. Matsui, M. Takeo, S. Negoro, T. Kanie, M. Katayama, and Y. Utsumi: Sens. Actuators A **145-146** (2008) 449.

[23] K. Matsui, I. Kawaji, Y. Utsumi, Y. Ukita, T. Asano, M. Takeo, D. Kato, and S. Negoro: J. Biosci. Bioeng. **104** (2007) 347.

[24] Y. Ukita, M. Kishihara, K. Kanda, S. Matsui, K. Mochiji, and Y. Utsumi: Jpn. J. Appl. Phys. **47** (2008) 337.

[25] K. Ikuta, A. Takahashi, K. Ikeda, and S. Maruo: Proc. MEMS 2003 (2003) 451.

[26] D. C. Duffy, J. C. McDonald, O. J. A. Schueller, and G. M. Whitesides: Anal. Chem. **70** (1998) 4974.

[27] Y. Kikutani, T. Horiuchi, K. Uchiyama, H. Hisamoto, M. Tokeshi, and T. Kitamori: Lab Chip **2** (2002) 188.

Figure captions

Figure 1 (a) Schematic illustration of DNA trapping and (b) fluorescence image of trapped DNA in triangular- microchannel.

Figure 2 (a) Schematic illustration of microchip fabrication procedure and (b) photograph of fabricated microchip.

Figure 3 Illustration of trapping experimental set-up.

Figure 4 Result of simulation (a) full view and (b) close-up view of highlighted part.

Figure 5 Fluorescence images of trapped DNA.

Figure 6 Time-shift of fluorescence intensity under conditions of (a) capillary type A with flow rate of 1.000 µl/min, (b) capillary type A with flow rate of 2.942 µl/min, and (c) capillary type C with flow rate of 1.000 µl/min.

Figure 7 Difference in trapping capacitance with applied voltage, capillary structure, and flow rate.

(a)

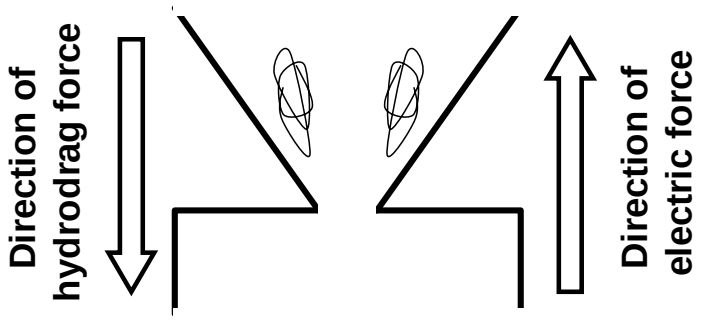

(b)

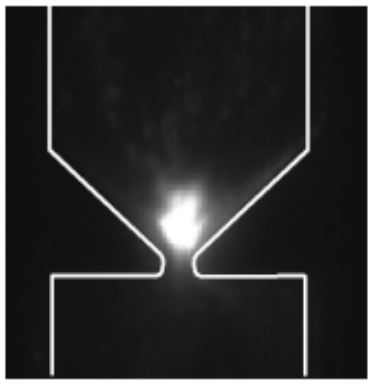

Fig. 1

(a)

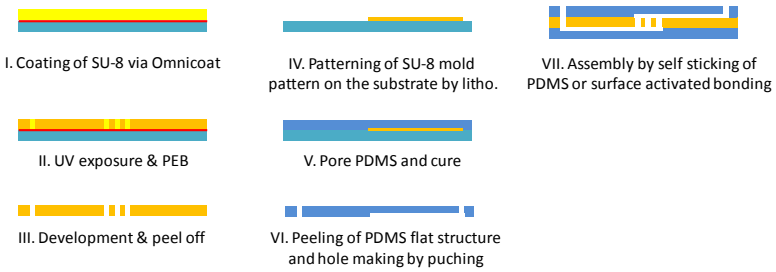
I. Coating of SU-8 via Omnicoat
II. UV exposure & PEB
III. Development & peel off
IV. Patterning of SU-8 mold pattern on the substrate by litho.
V. Pore PDMS and cure
VI. Peeling of PDMS flat structure and hole making by puching
VII. Assembly by self sticking of PDMS or surface activated bonding

(b)

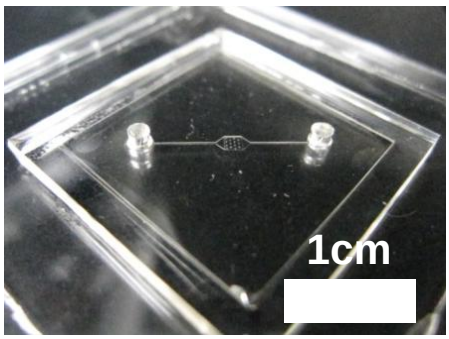
1cm

Fig. 2

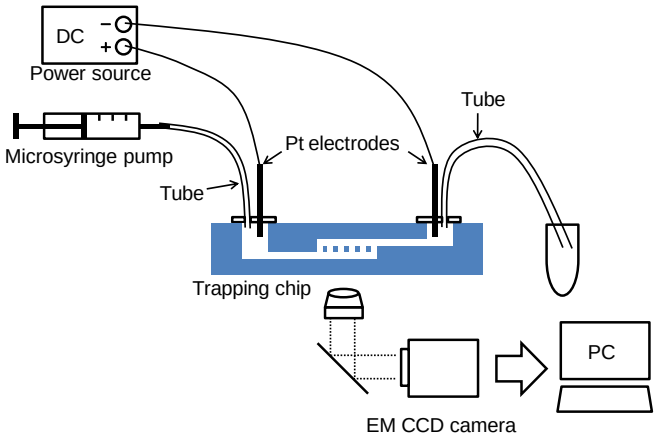
DC
−
+
Power source
Tube
Pt electrodes
Microsyringe pump
Tube
Trapping chip
PC
EM CCD camera

Fig. 3

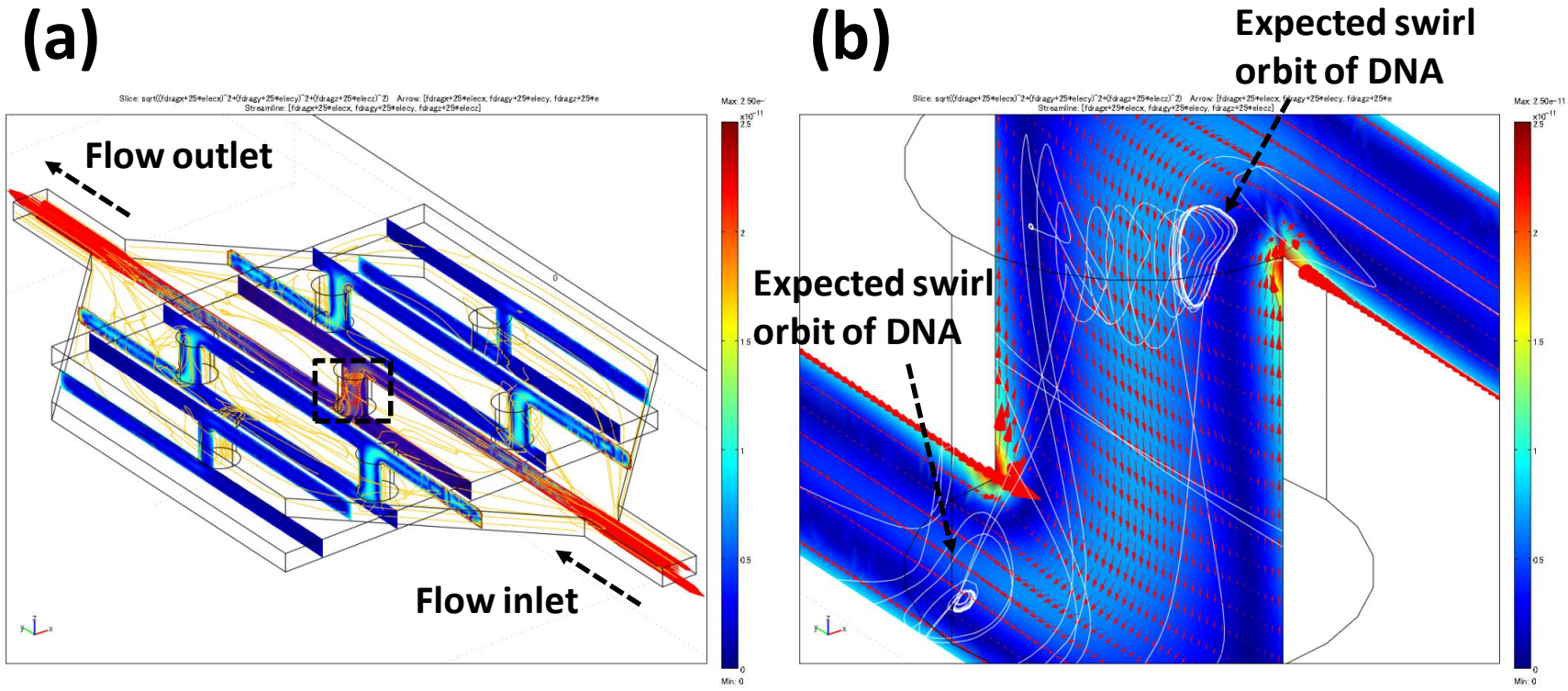
(a)
Flow outlet
Flow inlet
(b)
Expected swirl orbit of DNA
Expected swirl orbit of DNA

Fig. 4

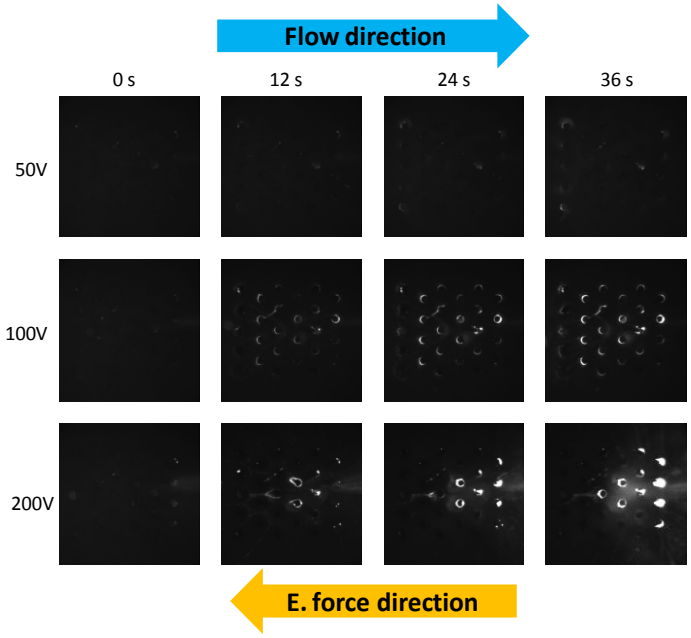
Flow direction
0 s
12 s
24 s
36 s
50V
100V
200V
E. force direction

Fig. 5

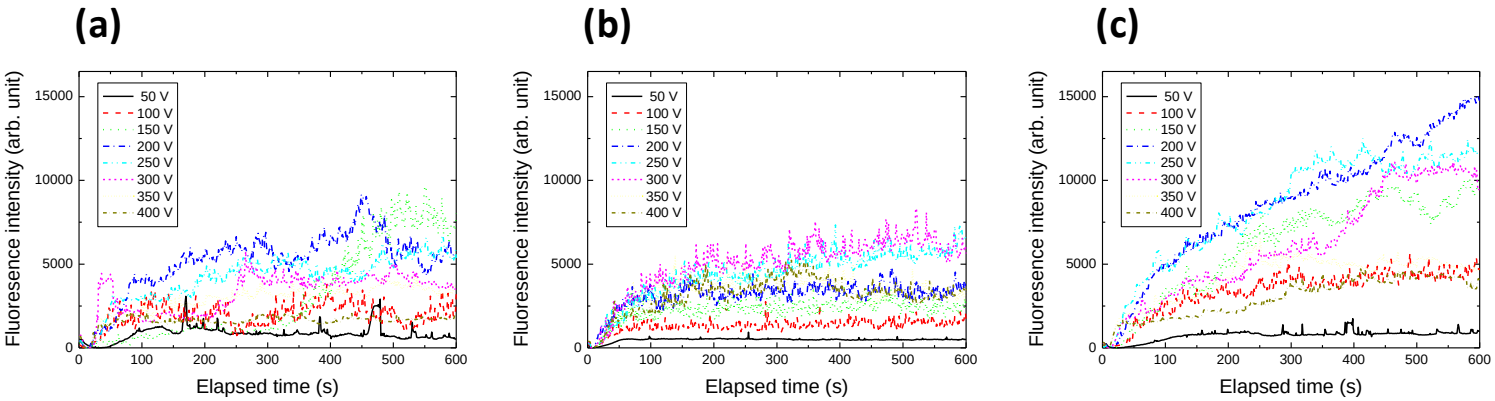
(a)
(b)
(c)
Fluorescence intensity (arb. unit)
Elapsed time (s)
50 V
100 V
150 V
200 V
250 V
300 V
350 V
400 V
0
5000
10000
15000
0
100
200
300
400
500
600

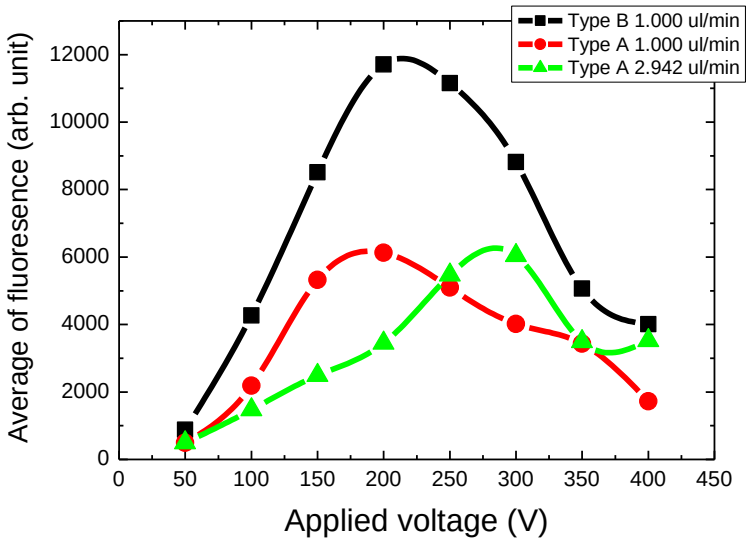
Type B 1.000 ul/min
Type A 1.000 ul/min
Type A 2.942 ul/min
Average of fluoresence (arb. unit)
0
2000
4000
6000
8000
10000
12000
0
50
100
150
200
250
300
350
400
450
Applied voltage (V)

Fig. 7